

An Experimental Investigation on the Breakup of Surfactant-Laden Shear-thinning Jets

A. Dechelette^{*1}, O. Campanella², C. Corvalan² and P.E. Sojka¹

¹Maurice J. Zucrow Laboratories, Department of Mechanical Engineering

²Department of Food Science

Purdue University

West Lafayette, IN 47907 USA

Abstract

The combined effect of polymers and soluble surfactants on the dynamics of jet breakup, and especially on satellite drop formation, was experimentally investigated. Xanthan gum and Carbopol® 934 NF were dissolved in water with Sodium Dodecyl Sulfate as the surfactant. Controlled disturbances were imposed at the laminar jet interface using a piezoelectric vibrating nozzle, and breakup dynamics were recorded using a high-speed camera. Drop and ligament diameters were measured from the digital images. The focus was on how bulk and interfacial properties of the prepared liquids influenced ligament and drop evolution. It was found that if the proper concentration of surfactant is selected, and if the flow time scales are large enough, Marangoni interfacial stresses develop and lead to an increase in satellite drop size. It was also confirmed that the introduction of surfactant contributes to a delay in jet breakup.

Introduction

Breakup of liquid jets has been a subject of fundamental importance in the optimization and control of such industrial spray processes as inkjet printing, tablet coating, spray drying, and in agricultural practices such as insecticides or fertilizer spraying. These processes often involve complex liquid formulations containing polymers and/or surface active agents (surfactants). Even though the dynamics of Newtonian capillary jet breakup has been widely studied [1-3], the behavior of non-Newtonian and/or surfactant covered jets is still a developing field. To date such jets have been studied experimentally using technique such as stroboscopy or high-speed imaging.

In regards to non-Newtonian jets, Gordon *et al.* [4] demonstrated that visco-elasticity suppresses formation of satellite drops, shortens the breakup length, and increases jet instability. Mun *et al.* [5] and Christanti and Walker [6-7] recently performed exhaustive experimental studies on breakup of jets formed by different molecular weight polyethylene oxide (PEO) solutions having the same viscosities. They found that polymers can be used to control satellite drop formation and that the addition of polymers also decreased the initial perturbation amplitude required to suppress the formation of satellites.

In parallel with these experiments, linear stability analyses were performed for visco-elastic jets. They require a rheological model for the non-Newtonian liquids. The Oldroyd B model was usually employed because of its convenience and generality. Key findings were that visco-elastic jets tend to be less stable than Newtonian jets under the same operating conditions [8], and that waves grow faster on visco-elastic jets resulting in shorter breakup lengths for weakly elastic liquids [9]. Based on these findings, Goren and Gottlieb [10] included an additional term in their linear dispersion equation that accounted for an unrelaxed axial tension in the jet. This led to definition of a non-dimensional elastic number (El). Doshi and Basaran [11] and Doshi *et al.* [12] used a slender filament 1-dimensional nonlinear analysis, while Renardy and Renardy [13] employed a 1-dimensional linear analysis to show that liquid filament dynamics near pinch-off follow a self-similar behavior for power law or Carreau fluids.

Numerical solutions confirmed the limitations arising from linear analysis: non-Newtonian jet breakup is a highly nonlinear phenomenon that cannot be accurately described by linearized equations. The Bousfield *et al* [14] numerical solution of visco-elastic breakup confirmed that the mechanism is controlled by the nonlinear (exponentially growing) extensional stresses, and Brenn *et al.* [15] confirmed that linear stability fails to accurately model visco-elastic jet breakup because of its inherent nonlinearity. It does, however, give good results for growth rate at low Weber number. More recently, Li and Fontelos [16] focused on drop dynamics of an Oldroyd-B liquid jet under the slender jet 1-dimensional assumption. Their approach accurately models drop drainage and coalescence usually observed in visco-elastic jet experiments. In addition, Dravid *et al.* [17] showed that the strength of shear-thinning, as characterized by the power law index n , strongly influences satellite drop formation dynamics for purely viscous Carreau fluid jets at low Reynolds number ($Re=5$); the stronger the shear-thinning, the smaller the satellite drop.

* Corresponding author: adechele@purdue.edu

Aside from polymeric fluid jet breakup, insoluble surfactant covered jets were studied by using either linear stability analysis [18-19] or nonlinear 1-dimensional slender jet approximation [19-20]. Hansen *et al.* [18] considered a surfactant covered Newtonian jet embedded in a viscous fluid, whereas Timmermans and Lister [19] considered liquid jets/threads in an inviscid environment. They both found that the presence of surfactant damps the growth rate of interfacial waves because of Marangoni stresses that arise from surfactant concentration gradients. Nonlinear one-dimensional approximation solutions provided insights into the dynamics involved in the drop formation process—Marangoni stresses were shown to contribute to a reduction in satellite drop size. These solutions are limited to dilute concentrations of surfactant. It was also shown that the self-similar solutions of Eggers [21-22] and Papageorgiou [23] are not affected by the presence of surfactant near breakup. This finding was confirmed by McCough and Basaran [24], who performed a 2-dimensional simulation of surfactant covered jets. They also found that surfactant initiates repetitive formation of thin threads between drops.

More recently, Dravid *et al.* [25] solved the full set of Navier-Stokes equations for viscous jets covered by insoluble surfactant. Marangoni effects were confirmed to be the cause of the satellite drop size reduction. In the same laboratory, Xue *et al.* [26], reported results from 2-dimensional simulations of shear-thinning liquid jets covered with insoluble surfactant. They demonstrated that surfactant can increase satellite drop development prior to breakup because of a competition between Marangoni stresses that reverse the flow into the liquid thread, and viscous forces that oppose the reversing flow. Recently Craster *et al.* [27] were the first to consider soluble surfactants in their nonlinear analysis. They concluded that soluble surfactant can actually enhance satellite drop size when present in concentrations above the critical micelle value (CMC).

Given the current state of understanding, this study focuses on how the combination of non-Newtonian rheological and surfactant addition affects filament/drop evolution. A soluble surfactant was used as it is not possible to accurately control the surface concentration of insoluble surfactants using our experimental system. This is not a significant weakness, however, because Campana and Saita [28] showed numerically that only the time scales of the two-phase flow dynamics differ between soluble and insoluble surfactant, the end result being the same. Comparisons between the results presented here and those from the only known study (numerical) on how rheology and surfactant presence affects jet breakup [26], is therefore possible.

The objectives of this study are to confirm the retarding effect of surfactant on the development of interfacial waves on a jet and to investigate the effect of surfactant on the dynamics of satellite drop formation: either satellite drop radius decreases, increases or does not change compared to surfactant free drops.

The following sections describe the experimental setup and process for preparing the liquids of interest, then present the effects of combining polymer and surfactant on filament/drop behavior. The dynamics of breakup are reported in terms of satellite drop sizes and filament breakup lengths as a function of perturbation wavenumber. Finally conclusions are presented, the limitations of this study noted, and future research areas suggested.

Materials and Methods

The fluids used to form filaments and drops are first routed through a gear pump (Micropump head GA-X21, Drive 500-4600 rpm) and then into a piezoelectric driven nozzle (University of Erlangen-Nürnberg, Germany). The nozzle has an orifice plate with a 200 μm diameter hole that is 13 μm thick (Melles-Griot). Jet breakup (Fig. 1) is recorded using a high-speed video camera (Phantom V7.1, Vision Research) at 14,285 fps. Proper illumination was achieved by directing the beam from a 500 W halogen lamp into a water container (for IR absorption) that was coupled to an optical diffuser. Room temperature was measured using a thermometer and found to be $22.5 \pm 0.5^\circ\text{C}$.

Shear-thinning liquids were prepared by adding Xanthan gum (Keltrol, CP Kelco) powder to de-ionized (DI) water, and allowing it to hydrate for 24 hr at 45°C . NaCl was then added to the water-XG solution and mixed for at least one hour using a magnetic stirrer. To reduce bacteriological growth in Xanthan-based mixtures, the solutions were stored at 4°C in air-tight containers and discarded after two to three weeks. Carbopol® 934 NF (Lubrizol) was also used. Powder was added to DI water and the solution was allowed to mix for 24 hours. At the end of mixing the solution was neutralized using NaOH, added in quantities of 0.4 g per gram of Carbopol® 934 NF, to prevent corrosion of the experimental system. Carbopol® is not subject to bacteriological growth, so no special storage care was required, provided that the containers are tightly closed to prevent water evaporation.

The effect of surfactant addition on the breakup process was investigated using SDS (Sodium Dodecyl Sulfate, SigmaUltra), an anionic surfactant that is widely used in personal care products, pharmaceutical products, agricultural sprays and other applications. For the surfactant to be efficient, its concentration must be close to the CMC (critical micelle concentration) in the solution of interest [29]. This is the concentration at which the Marangoni phenomenon takes place. For our formulations, SDS concentrations were chosen close to its CMC in water at 20°C , reported in the literature to be on the order of 0.2%. Three different concentrations of SDS were used: 0.1, 0.2 and 0.3%.

Rheological properties were measured using an ARG2 rotational rheometer (TA instruments) with a 60 mm diameter- 2° cone for shear rates ranging from 0.01 to $1,000 \text{ s}^{-1}$. Shear-thinning fluid parameters were obtained by fitting experimental data to the Carreau model:

$$\frac{\eta - \eta_{\infty}}{\eta_0 - \eta_{\infty}} = \left[1 + (\alpha \dot{\gamma})^2 \right]^{(n-1)/2} \quad (1)$$

where n is the power-law index [-], α is the consistency [s], η_0 is the zero-shear viscosity [Pa.s], η_{∞} is the infinite-shear-rate viscosity [Pa.s], and $\dot{\gamma}$ the shear rate [s^{-1}]. Small amplitude oscillatory strain (SAOS) measurements were also performed on each of the solutions and used to characterize liquid elasticity. Results are reported in terms of phase, δ , which is given by $\delta = \tan^{-1}(G''/G')$ where G'' is the loss modulus and G' is the elastic modulus of the liquid. δ larger than 45° corresponds to $G'' > G'$ (viscous dominated), while δ smaller than 45° corresponds to $G'' < G'$ (elastic dominated) [30].

Interfacial properties were measured using the Du Nouy ring method in both steady flow and oscillatory modes. However, it is important to note that the interfacial quantities measured may be affected by both the bulk and the interfacial rheological properties so they can only be used to compare solutions against with each other (no absolute quantities).

Filaments were formed using a square or sine wave of wavenumber $ka = 2\pi a/\lambda$ and voltage ± 200 V supplied to the piezo electric crystal. Here a is the nozzle radius [m] and λ is the disturbance wavelength [m]. A square wave was employed in order to achieve disturbance amplitudes large enough to be able to control the perturbation developing at the interface of Xanthan-based jets. In the case of Carbopol®-based jets, the amplitude reached by a sine wave was sufficient. To mimic real life applications, in which liquid formulations are modified but operating conditions are kept fixed, the pump speed was kept constant throughout the study.

Results and Discussion

In subsequent sections, the concentrations of NaCl (0.5%) in Xanthan-based liquids and of NaOH (0.04%) in Carbopol®-based liquids are not specified for convenience. The measured liquid properties and corresponding Reynolds numbers are presented in Table 1. Note also that diffusion coefficients (D) of SDS in water are reported to be $\sim 10^{-10}$ m²/s. This is an upper bound for this study since the presence of polymers and higher solution viscosities slows down the motion of surfactant molecules. $D \sim 10^{-10}$ m²/s corresponds to a diffusion time on the order of seconds considering the jet radius as a typical length scale. Breakup events are typically on the order of tens of milliseconds. This guarantees convection dominated molecular transport so surfactant concentration gradients are possible.

Effect of surfactant on rheology

As seen in Fig. 2.a and Fig. 2.b, addition of SDS to the Xanthan-NaCl solutions does not affect bulk rheology. However in the case of the Carbopol® 934 NF solutions, which are considered inelastic [4], addition of SDS considerably modifies both shear viscosity (Fig. 2.c) and phase, δ (Fig. 2.d)—there is a one order of magnitude decrease in zero-shear viscosity between 0 and 0.1% SDS, and slightly more than one order of magnitude between 0.2 and 0.3%. This decrease in viscosity is related to the interaction between SDS and Carbopol®. SDS addition increases the viscous-like behavior of Carbopol® mixtures over the range of frequencies considered.

Fig. 3.a and 3.b present interfacial shear viscosities measured using the du Nouy ring method. In the case of Xanthan-based liquids (Fig 3.a), a constant interfacial shear viscosity is achieved for an SDS concentration as low as 0.1%. In the case of Carbopol®-based liquids (Fig. 3.b), shear viscosity decreases to reach a constant profile for concentrations larger than 0.3%. This behavior can be explained using the mechanism responsible for the reduction of bulk shear viscosity. Interestingly, introduction of SDS leads to shear-thickening behavior of the interfacial viscosity.

Table 2 illustrates the effect of SDS addition on interfacial elasticity. When considering Table 2 entries, the addition of surfactant is seen to induce a decrease in δ for both Xanthan-based and Carbopol®-based liquids. This is consistent with an increase in interfacial elasticity. This increase in interfacial elasticity can be explained by the presence of surfactant at the interface. Ring oscillations displace surfactant molecules and give rise to a surfactant concentration gradient that leads to an interfacial force resisting ring motion, hence increasing apparent elasticity.

Effect of surfactant and rheology on jet breakup

Dimensionless breakup lengths are presented in Fig. 4 for Xanthan- and Carbopol®-based solutions. The data show that surfactant addition delays breakup for all concentrations, because its addition decreases the average surface tension and therefore reduces the growth rate of the interfacial capillary wave [19]. This results in an increase in jet breakup time. Adding surfactant above the CMC, however, yields no additional increase in breakup time. This is explained by the fact that the interface is saturated with surfactant molecules so the surfactant surface concentration no longer increases; this leads to a constant breakup length. The increased interfacial

elasticity associated with an increase in surfactant concentration (Table 2) also contributes to longer breakup lengths.

Prior to studying the effect of surfactant addition on satellite drop size, it is important to clearly understand the relationship between Marangoni stresses and surfactant concentration. At low concentration, there is not enough surfactant to create a sufficiently steep interfacial gradient, as seen in Fig. 5.a, and Marangoni stresses are insignificant. For an intermediate concentration (\sim CMC), there are enough surfactant molecules to create an interfacial gradient that is strong enough to produce a Marangoni stress; this will in turn increase satellite drop size (Fig. 5.b). Finally, a large concentration of surfactant (Fig. 5.c) prevents formation of an interfacial gradient and simply leads to a reduction in surface tension.

One typically wants to control drop size distributions during the spraying of pesticides or fertilizers. Surface active agents are often added to formulations so it is important to identify their effects on drop formation.

Dimensionless satellite drop radii are plotted versus dimensionless perturbation wavenumbers (ka) for different SDS concentrations and polymers in Fig. 6. Data for 0.2% SDS and 0.3% SDS Xanthan-based solution satellite drop sizes are presented at low wavenumbers only ($ka < 0.5$) because large concentrations of surfactant introduce the need for larger initial perturbation amplitudes in order to impose high frequencies. Such amplitudes cannot be generated using the current setup so conclusions for the full range of wavenumbers can only be drawn for 0% and 0.1% SDS jets.

The data show that the largest satellites are obtained for a concentration of 0.1% SDS. The same effect was observed by Xue *et al.* [26] for fully 2-dimensional simulations of insoluble surfactant covered shear-thinning jets, and is explained by considering Marangoni stresses (See Fig. 7). If the change of surfactant is assumed to be linear (a reasonable assumption for $R \ll \lambda$), the concentration gradient is:

$$\frac{d\gamma}{ds} \sim \frac{2(\gamma_{\max} - \gamma_{\min})}{\lambda} \quad (2)$$

At short wavelength, the gradient becomes large enough to influence satellite size, and is consistent with satellite drop size difference between 0.1 and 0% SDS being more significant at large wavenumber (100% increase at $ka \sim 0.7$).

In the case of Carbopol®, no significant effect of SDS on satellite formation is observed. This is related to the adsorption time of SDS compared to the breakup time of Carbopol® jets—there isn't enough time for all the surfactant to be adsorbed at the interface so the jets are like those of Fig. 5.a and no effect on satellite drop size is observed. This can also be explained by the enhancement of the satellite in the presence of surfactant being more pronounced for strong shear-thinning liquids [26]. The Carbopol®-based liquids presented here have a power law index between 0.73 and 0.90, whereas Xanthan-based liquids have a power law index of 0.47.

Conclusions

It was first shown that combinations of surfactants and polymers can significantly change the rheology of a mixture because of their ionic nature. The most fundamental effect was where an increase in surfactant concentration was shown to increase the interfacial elasticity and result in longer jet breakup lengths. It also led to slower perturbation wave growth rates because of lower average surface tension.

A second, and perhaps more significant finding, is confirmation of computer simulation results presented by Xue *et al.* [26]. Their predictions showed that surfactant addition can lead to an increase in satellite drop radius during the breakup of shear-thinning jets. This was observed here for Xanthan-SDS jets having a surfactant concentration close to the CMC. It is ascribed to Marangoni stresses that develop at the interface. In contrast, no effect on satellite formation was observed for weaker shear-thinning liquids (Carbopol®-based). This is due to either time scales involved for breakup that are shorter than surfactant adsorption times, or by the larger viscous forces that oppose Marangoni stresses.

References

- [1] Eggers, J., *Review of Modern Physics* 69(3):865-929 (1997).
- [2] Lin, S.P., and Reitz, R.D., *Annual Review of Fluid Mechanics* 30:85-105 (1998).
- [3] Eggers, J., and Villermaux, E., *Reports on Progress in Physics* 71:036601 (2008).
- [4] Gordon, M., Yerushalmi, J., and Shinnar, R., *Transactions of the Society of Rheology* 17:303-324 (1973).
- [5] Mun, R., Byars, J., and Boger, D., *Journal of Non-Newtonian Fluid Mechanics* 74:285-297 (1998).
- [6] Christanti, Y., and Walker, L., *Journal of Non-Newtonian Fluid Mechanics* 100:9-26 (2001).
- [7] Christanti, Y., Walker, L., *Journal of Rheology* 96:733-748 (2002).
- [8] Middleman, S., *Chemical Engineering Science* 20:1037-1040 (1965).
- [9] Goldin, M., Yerushalmi, J., Pfeffer, R., and Shinar, R., *Journal of Fluid Mechanics* 38:689-711 (1969).
- [10] Goren, S., Gottlieb, M., *Journal of Fluid Mechanics* 120:245-266 (1982).

- [11]Doshi, P., and Basaran, O.A., *Physics of Fluids* 16(3):585-593 (2004).
- [12]Doshi, P., Suryo, R., Yildirim, O.E., McKinley, and G.H., Basaran, O.A., *Journal of Non-Newtonian Fluid Mechanics* 113(1):1-27 (2003).
- [13]Renardy, M., and Renardy, Y., *Journal of Non-Newtonian Fluid Mechanics* 122:303-312 (2004).
- [14]Bousfield, D.W., Keunings, R., Marrucci, G., and Denn, M.M., *Journal of NN Fluid Mechanics* 21:79-97 (1986).
- [15]Brenn, G., Liu, Z., and Durst, F., *International Journal of Multiphase Flow* 26:1621-1644 (2000).
- [16]Li, J., Fontelos, M.A., 2003. Drop dynamics of the beads-on-string structure. *Physics of Fluids* 15(4), 922-937.
- [17]Dravid, V., Loke, P.B., Corvalan, C.M., and Sojka, P.E., *Journal of Fluids Engineering* 130:081504 (2008).
- [18]Hansen, S., Peters, G.W.M., and Meijer, H.E.H., *Journal of Fluid Mechanics* 382:331-349 (1999).
- [19]Timmermans, M.-L.E., and Lister, J.R., *Journal of Fluid Mechanics* 459:289-306 (2002).
- [20]Craster, R.V., Matar, O.K., and Papageorgiou, D.T., *Physics of Fluids* 14(4):1364-1376 (2002).
- [21]Eggers, J., *Physical Review Letters* 71(21):3458-3460 (1993).
- [22]Eggers, J., *Physics of Fluids* 7(5):941-953 (1994).
- [23]Papageorgiou, D., *Physics of Fluids* 7:1529-1544 (1995).
- [24]McCough, P.T., and Basaran, O.A., *Physical Review Letters* 96:054505 (2006).
- [25]Dravid, V., Songsermpong, S., Xue, Z., Corvalan, C.M., and Sojka, P.E., *Chemical Engineering Science* 61:3577-3585 (2006).
- [26]Xue, Z., Corvalan, C.M., Dravid, V., and Sojka, P.E., *Chemical Engineering Science* 63:1842-1849 (2008).
- [27]Craster, R.V., Matar, O.K., and Papageorgiou, D.T., *Journal of Fluid Mechanics* 629:195-219 (2009).
- [28]Campana, D.M., and Saita, F.A., *Physics of Fluids* 18(2):022104 (2006).
- [29]Tadros, T.F., *Applied Surfactants: Principles and Applications*, first ed. WILEY-VCH Verlag GmbH & Co. KGaA (2005).
- [30]Morrison, F.A., *Understanding Rheology*, Oxford University Press (2001).

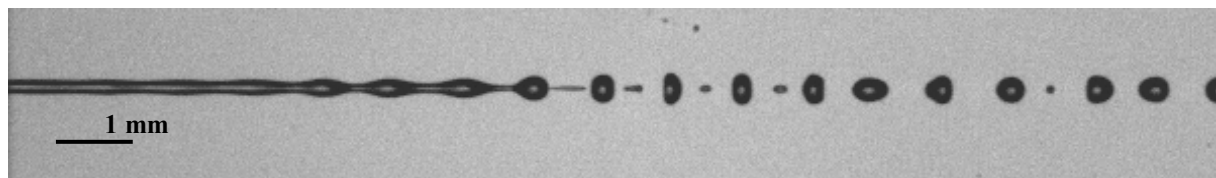
Table 1. Measured liquid properties.

Formulation	η_0 [mPa.s]	η_∞ [mPa.s]	n [-]	α [s]	σ_{eq}^1 [mN/m]	ρ [kg/m ³]	$Re_0 = \frac{\rho a U}{\eta_0}$
0.1% XG 0% SDS	222.1 ± 4.4	(6.7 ± 0.1) x10 ⁻¹	0.47 ± 0.01	3.7 ± 0.1	69.4 ± 0.2	996 ± 5	2.6 ± 0.2
0.1% XG 0.1% SDS	251.6 ± 5.0	(6.2 ± 0.1) x10 ⁻¹	0.47 ± 0.01	4.7 ± 0.1	38.6 ± 0.2	993 ± 5	2.3 ± 0.2
0.1% XG 0.2% SDS	238.8 ± 4.6	(7.1 ± 0.1) x10 ⁻¹	0.47 ± 0.01	4.2 ± 0.1	38.2 ± 0.1	992 ± 5	2.4 ± 0.2
0.1% XG 0.3% SDS	275.6 ± 4.2	(6.7 ± 0.1) x10 ⁻¹	0.47 ± 0.1	5.3 ± 0.1	38.3 ± 0.2	994 ± 5	2.1 ± 0.2
0.1% Carbopol® 0% SDS	151.2 ± 3.2	(6.0 ± 0.1) x10 ⁻⁶	0.73 ± 0.02	4.5 ± 0.1	73.7 ± 0.2	990 ± 5	3.5 ± 0.3
0.1% Carbopol® 0.1% SDS	14.7 ± 1.1	(5.4 ± 0.4) x10 ⁻⁵	0.86 ± 0.07	(2.7 ± 0.2) x10 ⁻¹	40.9 ± 0.5	985 ± 5	35.6 ± 4.0
0.1% Carbopol® 0.2% SDS	7.3 ± 0.3	(1.9 ± 0.1) x10 ⁻⁴	0.90 ± 0.04	(1.6 ± 0.1) x10 ⁻¹	41.1 ± 0.1	992 ± 5	72.1 ± 6.7
0.1% Carbopol® 0.3% SDS	7.9 ± 0.5	(6.9 ± 0.4) x10 ⁻³	0.90 ± 0.05	(1.2 ± 0.1) x10 ⁻¹	42.3 ± 0.3	992 ± 5	66.6 ± 7.0

¹Equilibrium surface tension; not the surface tension during jet breakup.

Table 2. Averaged interfacial phase delta for Xanthan-based liquids and Carbopol[®]-based liquids over frequency range 0.01 s^{-1} to 1 s^{-1} .

Formulation	δ [deg]
0.1% XG 0% SDS	46.0 ± 7.1
0.1% XG 0.1% SDS	37.2 ± 12
0.1% XG 0.2% SDS	32.4 ± 7.4
0.1% XG 0.3% SDS	28.2 ± 4.9
0.1% Carbopol [®] 0% SDS	28.4 ± 4.2
0.1% Carbopol [®] 0.1% SDS	21.3 ± 13
0.1% Carbopol [®] 0.2% SDS	14.0 ± 4.0
0.1% Carbopol [®] 0.3% SDS	11.4 ± 2.5

**Figure 1.** Breakup of a jet of 0.1% Carbopol[®] and 0.1% SDS at $Re_0=3.5$

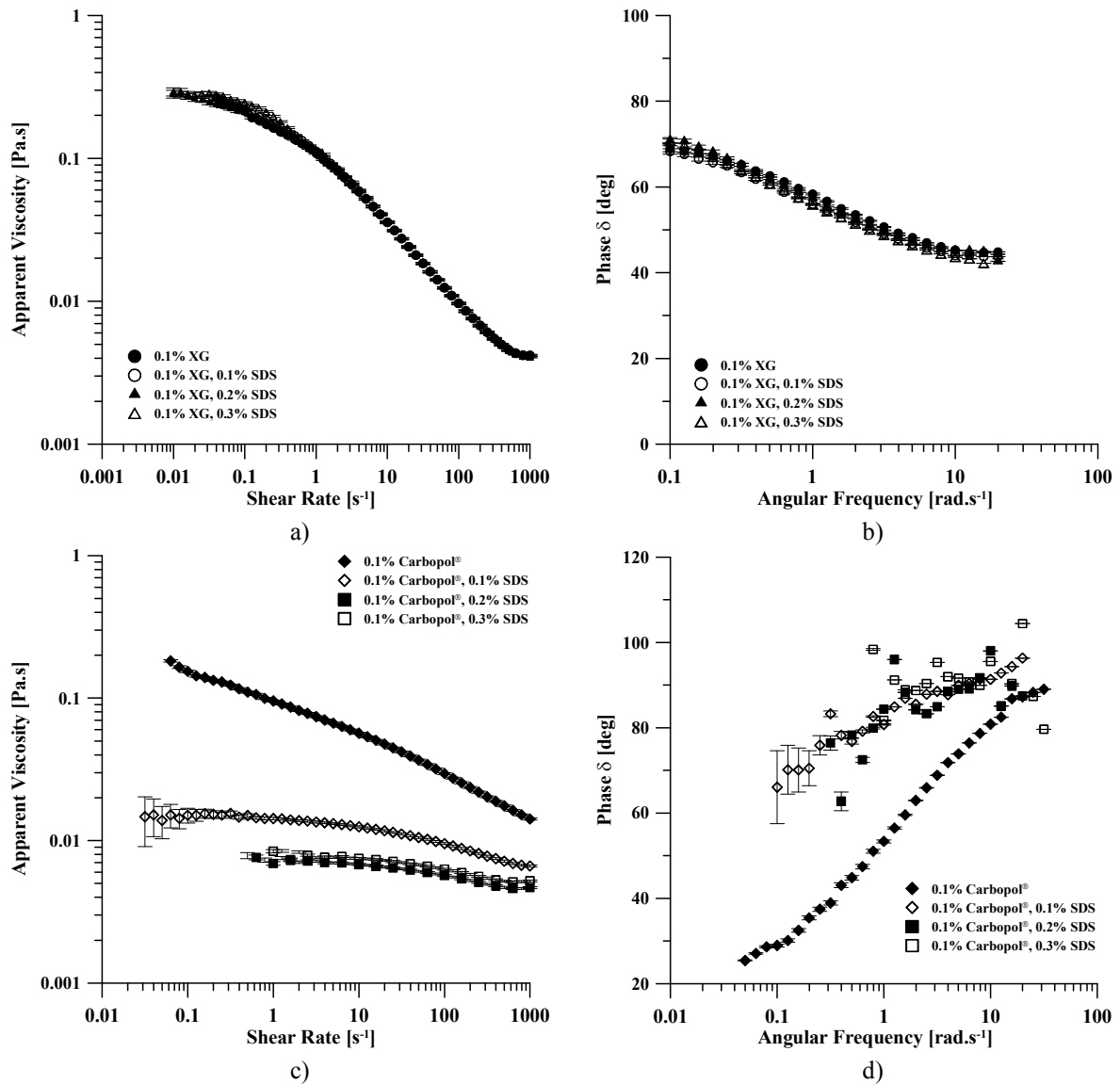


Figure 2. a) Shear viscosity versus shear rate for Xanthan-based solutions measured at T=22.5°C, b) Phase versus angular frequency in SAOS measurements of Xanthan-based solutions measured at strain $\gamma = 0.1$ and T=22.5°C, c) Shear viscosity versus shear rate for Carbopol[®]-based solutions measured at T=22.5°C, and d) Phase versus angular frequency in SAOS measurements of Carbopol[®]-based solutions measured at strain $\gamma = 0.1$ and T=22.5°C.

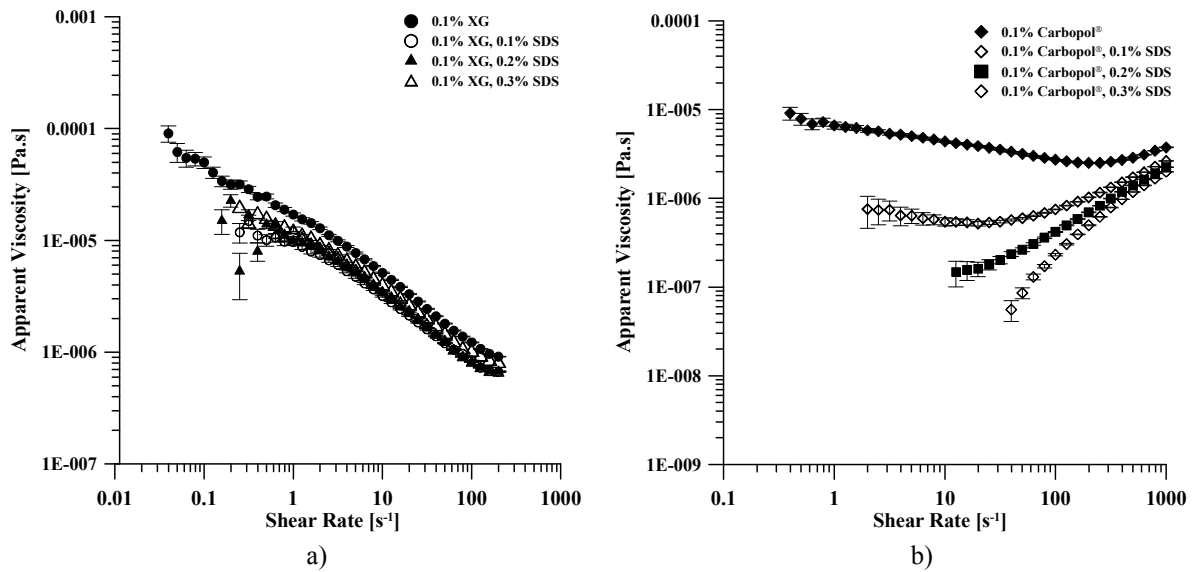


Figure 3. a) Interfacial shear viscosity versus shear rate for Xanthan-based solutions measured at torque $M=0.01$ nN.m and $T=22.5^{\circ}\text{C}$ and b) Interfacial shear viscosity versus shear rate for Carbopol[®]-based solutions measured at torque $M=0.01$ nN.m and $T=22.5^{\circ}\text{C}$.

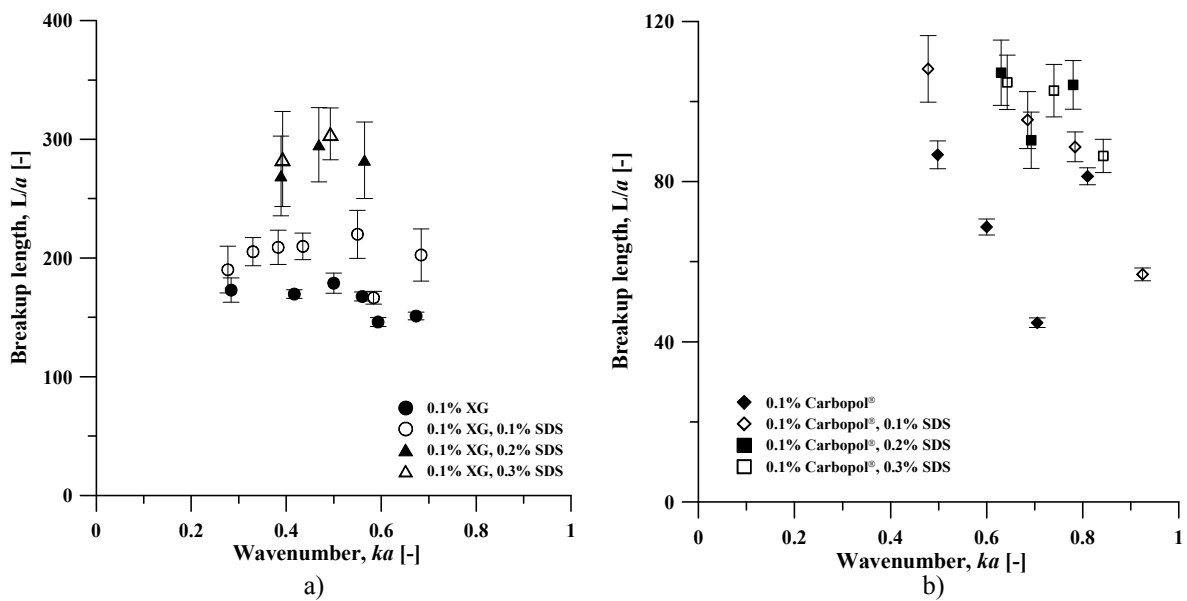


Figure 4. Dimensionless breakup length versus dimensionless wavenumber for a) Xanthan-based solutions and b) Carbopol[®]-based solutions.

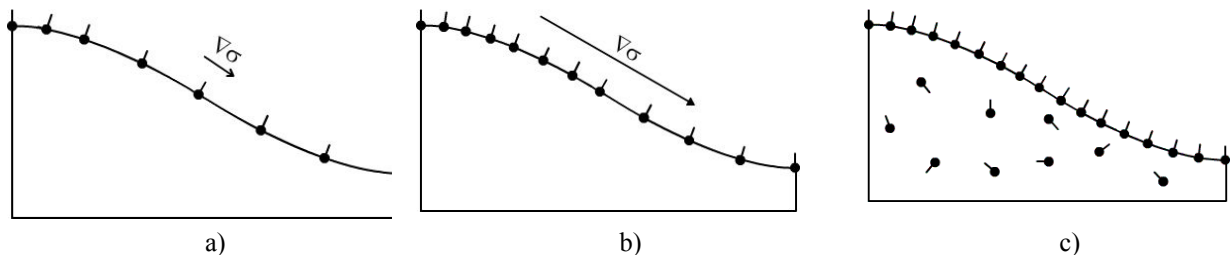


Figure 5. Marangoni effect for a) low surfactant concentration, b) medium surfactant concentration, c) high surfactant concentration (presented for half a wavelength)

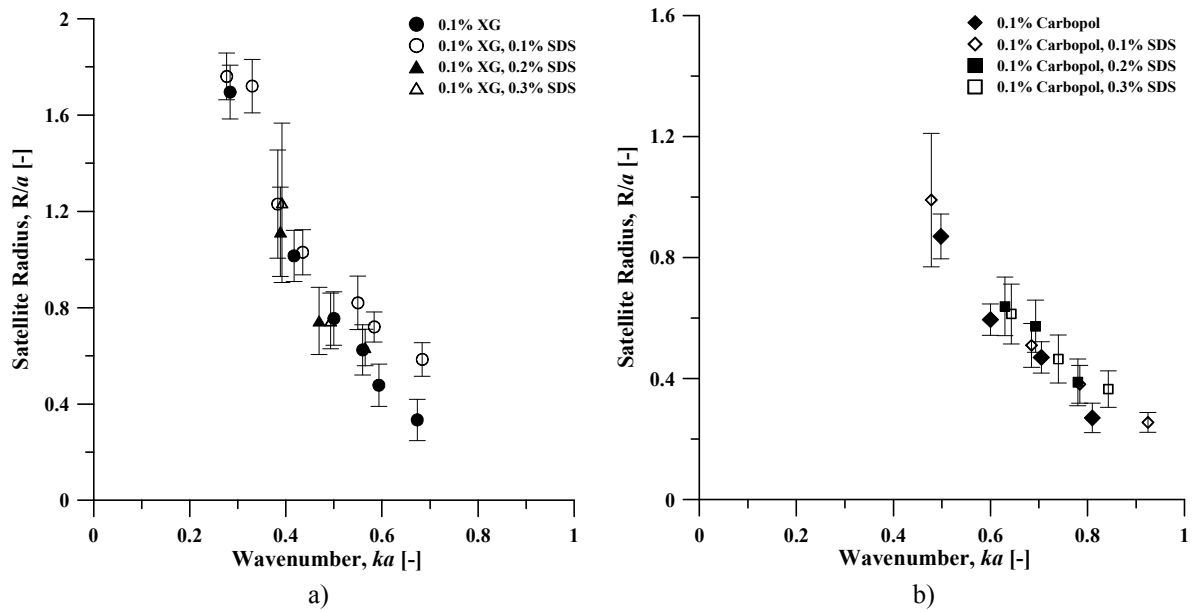


Figure 6. Dimensionless satellite drop radius versus dimensionless wavenumber for a) Xanthan-based solutions and b) Carbopol®-based solutions.

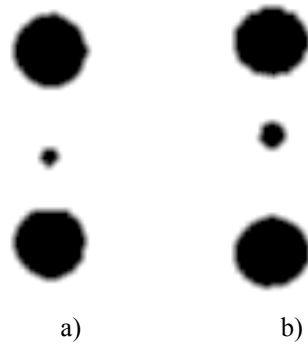


Figure 7. Close-up view to illustrate surfactant effect on satellite drop size a) 0.1% XG, 0% SDS at $ka=0.67$ and b) 0.1% XG, 0.1% SDS at $ka=0.68$ (pictures have same scale and have been enhanced using digital filters).